Discovery of Potent and Muscle Selective Androgen Receptor Modulators through Scaffold Modifications

James J. Li,[||,*] James C. Sutton,[||,§] Alexandra Nirschl,[||] Yan Zou,[||] Haixia Wang,[||] Chongqing Sun,[||] Zulan Pi,[||] Rebecca Johnson,[||,‡] Stanley R. Krystek, Jr.,[⊥] Ramakrishna Seethala,[⊗] Rajasree Golla,[⊗] Paul G. Sleph,[⊗] Blake C. Beehler,[⊗] Gary J. Grover,[⊗,†] Aberra Fura,[#] Viral P. Vyas,[#] Cindy Y. Li,[@] Jack Z. Gougoutas,[▽] Michael A. Galella,[▽] Robert Zahler,[||] Jacek Ostrowski,[⊗] and Lawrence G. Hamann[||]

Discovery Chemistry, Computer Assisted Drug Design, Metabolic Disease Research, Metabolism and Pharmacokinetics, Discovery Analytical Sciences, and Analytical Research and Development, Bristol-Myers Squibb Pharmaceutical Research Institute, P.O. Box 5400, Princeton, New Jersey 08543-5400

Received March 19, 2007

A novel series of imidazolin-2-ones were designed and synthesized as highly potent, orally active and muscle selective androgen receptor modulators (SARMs), with most of the compounds exhibiting low nM in vitro potency in androgen receptor (AR) binding and functional assays. Once daily oral treatment with the lead compound **11a** (AR K_i = 0.9 nM, EC_{50} = 1.8 nM) for 14 days induced muscle growth with an ED_{50} of 0.09 mg/kg, providing approximately 50-fold selectivity over prostate growth in an orchidectomized rat model. Pharmacokinetic studies in rats demonstrated that the lead compound **11a** had oral bioavailability of 65% and a plasma half-life of 5.5 h. On the basis of their preclinical profiles, the SARMs in this series are expected to provide beneficial anabolic effects on muscle with minimal androgenic effects on prostate tissue.

Introduction

As men age beyond the third decade of life, they experience a slow steady decrease in serum testosterone levels.[1] The physiological impact of testosterone decline in elderly men is associated with reduced muscle mass and strength, decreased bone mass, low energy, diminished sexual function, an increased risk of osteoporosis and fracture, and an increased incidence of depression, all of which can have a significant negative impact on quality of life.[2−4] Testosterone replacement therapy (TRT)[a] has been shown in clinical studies to significantly increase lean body mass and bone density, decrease adipose tissue, and in some studies, increase muscle strength.[5−9] However, the use of long-term TRT is limited, mainly due to concerns about accelerating benign prostatic hypertrophy (BPH) and/or prostate cancer.[10−11] As such, there exists considerable unmet medical need for a novel therapy that would retain the beneficial anabolic effects on muscle and bone with minimal androgenic effects on prostate. Consequently, discovery of an orally active, nonsteroidal, and selective androgen receptor modulator (SARM) continues to be an area of high interest among the biomedical research community.[12−18] Several distinct series of orally active compounds such as **1** (LG-121071), **2** (S-4), **3** (BMS-564929), **4** (LGD-2226), **5**, and **6** have been reported in the literature (Figure 1).[19−36] As compared to endogenous testosterone, these new agents have demonstrated, to varying degrees, potent and efficacious anabolic activity on muscle and/or bone with significantly improved selectivity versus prostate in preclinical rodent models and therefore have the potential to provide safer treatment options with fewer side-effects as compared to conventional TRT.

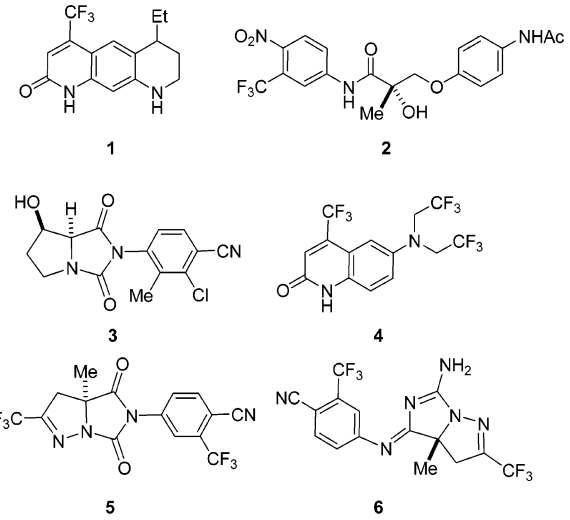

Figure 1. Representative examples of nonsteroidal androgen agonists.

As reported recently by our group, *N*-aryl hydroxybicyclohydantoin **3** is as an orally active, highly potent SARM that had advanced to clinical studies.[28] Most of our first generation SARMs, including **3**, have a hydantoin moiety embedded within the [5.5] bicyclic scaffold.[28−30] During the course of structure−activity relationship (SAR) optimization, a trace amount of the potentially mutagenic 4-cyanonaphtylamine metabolite was detected in dog and cynomolgus monkey urine upon oral dosing of early lead compound **7** (Table 1).[29] Two complementary approaches were taken to circumvent this issue. The first focused on the evaluation of various alternative aryl amines. This

* Corresponding author: Telephone: 609-818-7124, e-mail: James.Li@bms.com.
[||] Discovery Chemistry.
[⊥] Computer Assisted Drug Design.
[⊗] Metabolic Disease Research.
[#] Metabolism and Pharmacokinetics.
[@] Discovery Analytical Sciences.
[▽] Analytical Research and Development.
[§] Current address: Novartis Institutes of Biomedical Research, 4560 Horton St., Emeryville, CA 94608. email: james.sutton@novartis.com.
[‡] Current address: Department of Defense, 200 MacDill Blvd., Washington, D.C. 20340. e-mail: rejohns@dia.mil.
[†] Current address: Product Safety Laboratories, 2394 Rt. 130, Dayton, NJ 08810. email: garygrover@productsafetylabs.com.

[a] Abbreviations: SARM, selective androgen receptor modulator; AR, androgen receptor; TRT, testosterone replacement therapy; BPH, benign prostatic hypertrophy; LBD, ligand binding domain; ADME, absorption, distribution, metabolism, and excretion; DHT, dihydrotestosterone; IA, intrinsic activity.

10.1021/jm070312d CCC: $37.00
Published on Web 06/07/2007

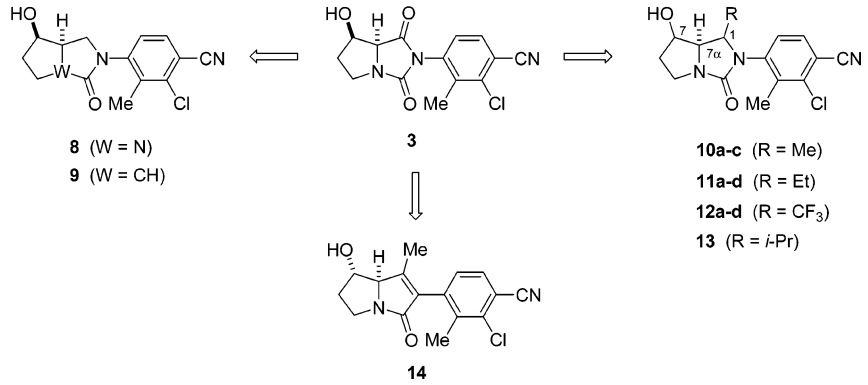

Figure 2. Overall strategy for hydantoin core modification from lead **3**.

Scheme 1[a]

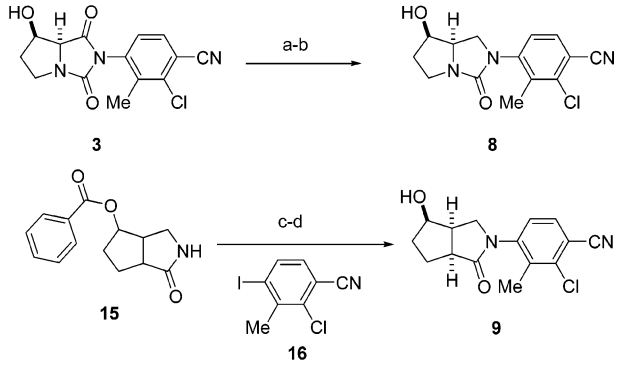

[a] Reagents and conditions: (a) $LiEt_3BH$, −78 °C; (b) Et_3SiH, BF_3Et_2O, −78 °C to 0 °C, 6%; (c) CuI, K_3PO_4, 1,2-cyclohexyldiamine, 21%; (d) 1 M KOH, 88%.

approach led to the successful identification and incorporation of the nonmutagenic 3-chloro-4-cyano-2-methylaniline moiety to provide compound **3**, which surpasses the highly potent and muscle selective AR agonist profile of earlier leads.[30] In parallel to the search for nonmutagenic aryl amine replacements, a second approach entailing systematic modification of the hydantoin core structure to reduce the likelihood of aryl amine release (Figure 2) was also undertaken. Throughout these efforts, both the optimized [5.5] bicyclic scaffold and the newly discovered 3-chloro-4-cyano-2-methylphen-1-yl group were retained as the key pharmacophoric features for potent AR binding and functional activity. Herein we wish to report the results of these scaffold modification efforts, leading to the identification of advanced preclinical candidates (such as **11a**) with favorable pharmaceutics properties.

Chemistry

The primary objective of the hydantoin core modifications (Figure 2) was to minimize the potential for aryl amine release in vivo while maintaining potent SARM activity. Conceptually, these modifications included replacement of one of the two potentially labile *N*-acyl bonds of **3** with an alternative *N*-alkyl fragment as in compounds **8**−**13**, as well as obviation of an aniline fragment altogether as in **14**. Toward that end, general synthetic approaches for preparation of the scaffolds in compounds **8** to **14** were developed using **3** or other available advanced intermediates as outlined in Schemes 1−4. Reduction of the amide carbonyl in **3** was achieved by a two-step sequence as an expedient entry to the des-oxo compound **8**. Pyrrolidin-2-one **9** was prepared by a copper(I)-catalyzed *N*-arylation of **15**[37] with **16**, followed by two sequential chromatographic separations on ChiralPak AD and OD columns, and removal of benzoyl ester protecting group to provide **9** as single enantiomer. The absolute stereochemistry of **9** was determined by single-crystal X-ray crystallography.

Simple methyl- and ethyl-substituted imidazolidin-2-one analogues **10a**−**c** and **11a**−**d** were prepared from *N*-Boc pyrrolidine aldehyde **17a** (Scheme 2). Reaction of methyl- or ethylmagnesium bromide with **17a** gave the corresponding diastereomeric alcohols **18a**,**b**, which were then oxidized with 4-methyl morpholine *N*-oxide (NMO) in the presence of catalytic tetrapropylammonium perruthenate (TPAP) to provide ketone **19**. Treatment of **19** with hydroxylamine gave the oxime intermediate which was hydrogenated to furnish amine **20a** as the only diastereomer isolated. *N*-Arylation of **20a** with **16** under Buchwald conditions[38] provided aniline **21**. Removal of *N*-Boc protecting group in **21**, followed by reaction with phosgene, provided the *tert*-butyldimethylsilyl (TBS)-protected **10a** or **11a**. The TBS group was then removed by treatment with tetrabutylammonium fluoride (TBAF) to give compounds **10a** and **11a**. Alternatively, diastereomeric alcohols **18a** and **18b** could be separated by silica gel chromatography, and the first eluting isomer **18a** was allowed to react with methanesulfonyl chloride to form a mesylate intermediate. Azide displacement of the mesylate group, followed by reduction of the resulting azo intermediate, gave diastereomeric amine **20b**. With **20b** in hand, it was readily converted to **10b** or **11b** in a similar manner. With respect to the 7-hydroxyl diastereomers **10c**, **11c**, or **11d**, they were prepared via Mitsunobu reaction from **10a**, **11a**, or **11b**, respectively, to give the benzoyl ester intermediates. Hydrolysis of the resulting respective benzoyl esters under basic conditions provided the isomers **10c**, **11c**, and **11d**.

Trifluoromethyl-substituted imidazolidin-2-one analogues **12a**−**d** were prepared employing a slightly different cyclization strategy (Scheme 3). Cesium fluoride-mediated trifluoromethyl addition to **17b** provided diastereomeric alcohols **22a**,**b,** which were readily separated and carried forward individually. Removal of the *N*-Boc group of **22a**, followed by reaction with isocyanate **23**, provided urea intermediate **24a**. Treatment of **24a** with potassium *tert*-butoxide and *p*-toluenesulfonyl chloride afforded compound **12d** after removal of TBS group. Likewise, compound **12c** was prepared from alcohol **22b**, and **12a**,**b** from aldehyde **17a** as shown in Scheme 3. It was later found that compound **11a** could also be prepared from **18b** (R = Et) using conditions described in steps b−e of Scheme 3, giving an improved overall yield. Furthermore, alcohol isomer **18a** (R = Et) can be converted to **18b** (R = Et) in a two-step sequence involving Mitsunobu inversion followed by hydrolysis of the resulting ester as shown in steps l and m of Scheme 2. The stereochemistry of these alkyl-substituted imidazolidinones

Scheme 2[a]

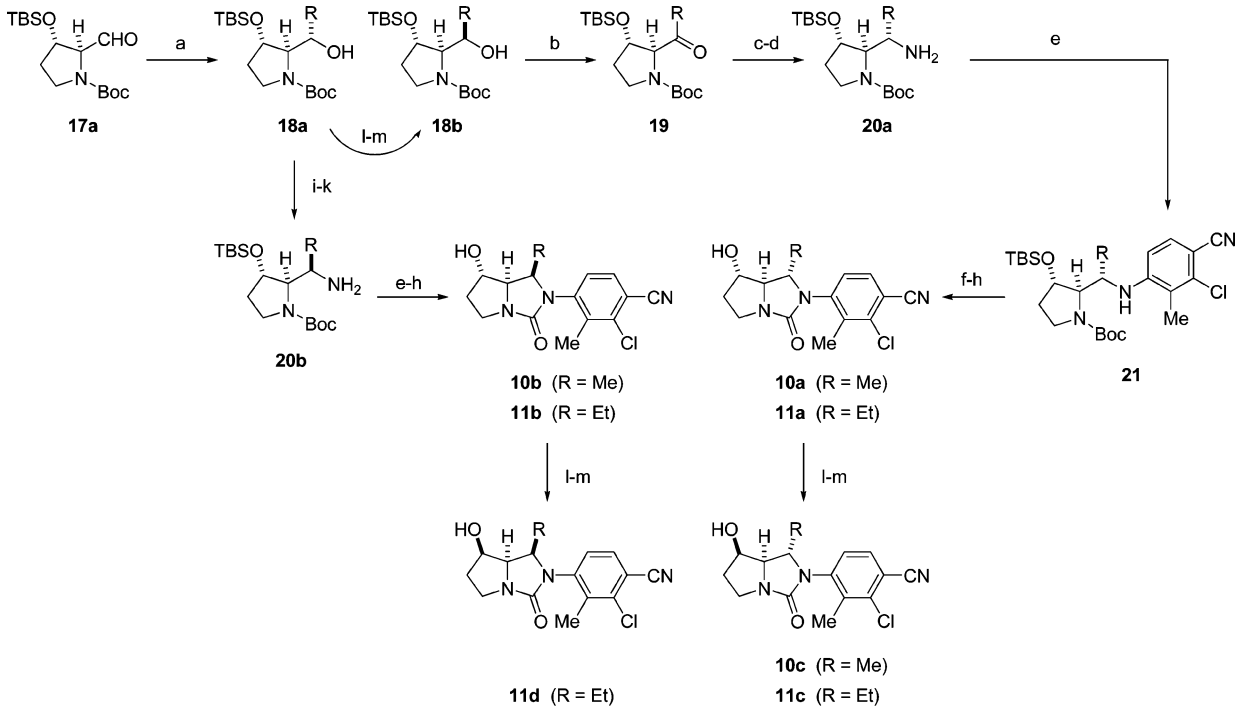

[a] Reagents and conditions: (a) MeMgBr or EtMgBr, −60 to −78 °C, 50−60%; (b) NMO, *n*-Pr_4NRuO_4, 87%; (c) NH_2OHHCl, NaOAc, ∼98%; (d) H_2, Raney Ni, 10% Pd/C, 95%; (e) compd **16**, $Pd_2(dba)_3$, (*R*)-*N*,*N*-dimethyl-1-[(*R*)-2-(diphenyphosphino)ferrocenyl]-ethylamine, Cs_2CO_3, 21%; (f) 15% TFA/CH_2Cl_2; (g) $COCl_2$, *i*-Pr_2NEt, 86%; (h) Bu_4NF, 68%; (i) $MeSO_2Cl$, *i*-Pr_2NEt, DMAP, 78%; (j) NaN_3, 77%; (k) H_2, 5% Pd/C, 98%; (l) $PhCO_2H$, Ph_3P, diisopropyl azodicarboxylate, 94%; (m) 1 N NaOH, 88%.

Scheme 3[a]

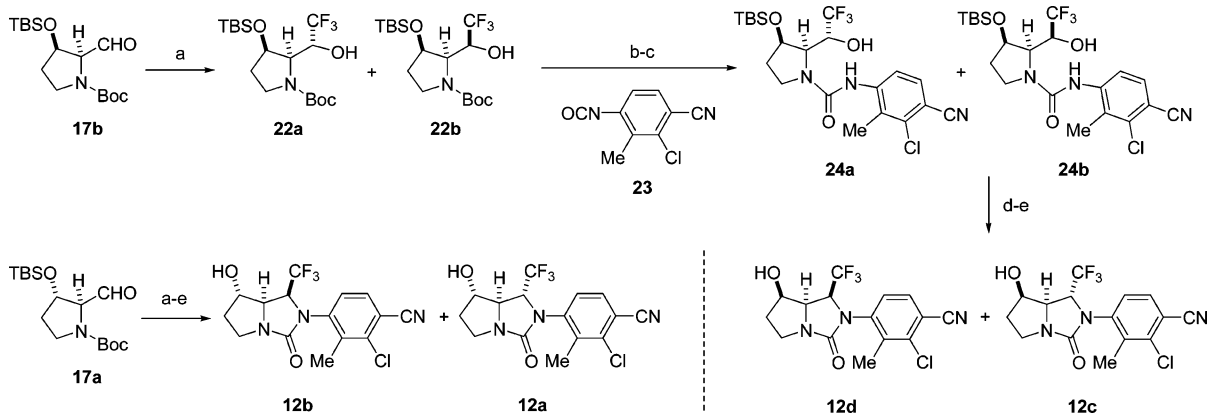

[a] Reagents and conditions: (a) CF_3SiMe_3, CsF, isomers separated and carried forward individually, 50% and 8%; (b) ∼30% TFA/CH_2Cl_2; (c) *i*-Pr_2NEt, 93%; (d) *tert*-BuOK, *p*-$TolSO_2Cl$, 69%; (e) Bu_4NF, 86%.

Scheme 4[a]

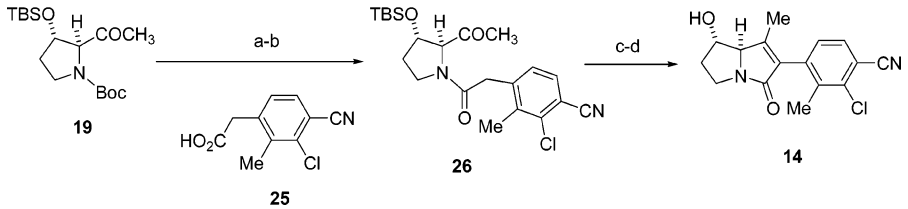

[a] Reagents and conditions: (a) 10% TFA/CH_2Cl_2; (b) PyBroP, *i*-Pr_2NEt, 36%; (c) piperidine, 7%; (d) HF pyridine, 73%.

10a−**c**, **11a**−**d**, and **12a**−**d** were confirmed by NOE analysis, and in the case of **12d**, by X-ray crystal structural analysis.

The aniline nitrogen replacement analogue pyrrol-2-one **14** was prepared from ketone **19** (Scheme 4). Deprotection of the *N*-Boc group in **19**, followed by amide formation with acid **25** in the presence of bromo tris-(pyrrolidinophosphonium) hexafluorophosphate (PyBroP), provided amide intermediate **26**. Piperidine-assisted intramolecular cyclization, followed by removal of the TBS group with HF-pyridine, provided pyrrol-2-one **14**.

Biological Results and Discussion

Our previous SAR investigations demonstrated a strong preference for a [5.5] fused bicyclic scaffold substituted with a 3-chloro-4-cyano-2-methylphenyl moiety for potent and muscle

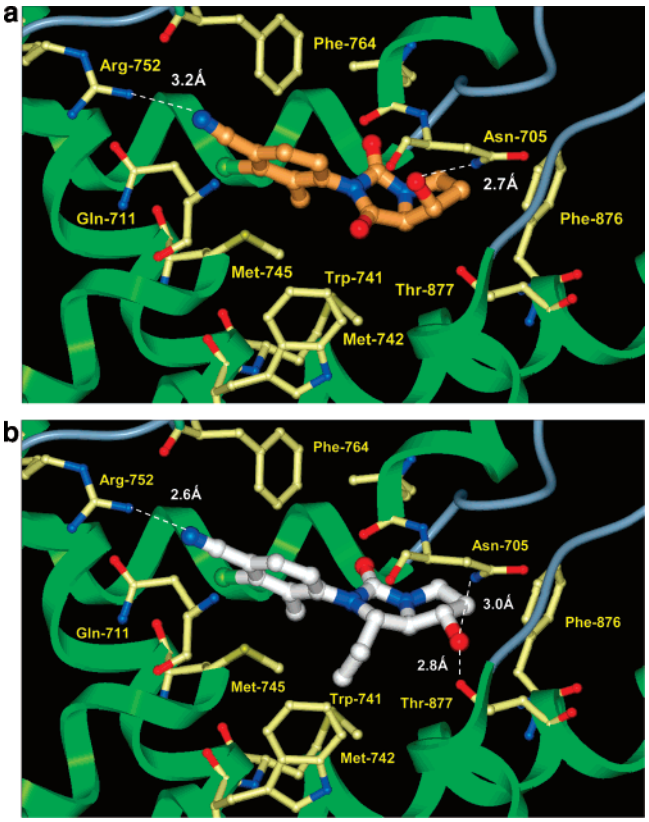

Figure 3. (**a**) X-ray cocrystal structure of **3** bound to the human androgen receptor ligand binding domain at 3.0 Å resolution. Key residues in the active site are displayed and colored by atom type (C, beige, N blue, O red). Dashed lines indicate potential hydrogen bonds with distance between heavy atoms shown. A portion of the backbone green ribbon was removed for clarity. (**b**) Docking model of **11a** in human androgen receptor ligand binding domain. Key residues in the active site are displayed and colored by atom type (C, white, N blue, O red). Key contacts are a bifurcated hydrogen bond between hydroxyl group to Asn-705 and Thr-877, and cyano group with Arg-752. Dashed lines indicate potential hydrogen bonds with distance between heavy atoms shown. The π-edge−face interaction of aryl ring with Phe-764 also provides another key interaction. A portion of the backbone green ribbon was removed for clarity.

selective in vivo activity.[28−30] Modification to either the corresponding [5.6] or [6.5] bicyclic ring systems resulted in a dramatic loss of activity.[39] Analysis of the X-ray cocrystal structure of compound **3** bound to the AR ligand binding domain (LBD) reveals some key interactions within the binding site (Figure 3a).[28] There are hydrogen bonds between the 7-hydroxyl and aryl nitrile groups of compound **3** to Asn-705 (2.7 Å) and Arg-752 (3.2 Å), respectively, and a π-edge-face interaction of the aryl group of **3** with Phe-764. In addition, it is noted that there are no direct contacts for the amide carbonyl group of the hydantoin ring with residues in the binding site. This carbonyl is projected instead to a small hydrophobic cavity surrounded by the Trp-741, Met-742, and Met-745 residues. The dihedral angle between the aryl group and the hydantoin ring is 62°, which appears to provide an optimal conformation to ensure that key interactions are achieved within the binding pocket. Proton NMR analysis of compound **3** also indicates there are two distinguishable rotamers around the *N*-aryl bond, which are interconvertible. Taken together these data suggest a small hydrophobic group in place of the amide carbonyl may fit in the hydrophobic pocket and induce a similar conformational arrangement. Furthermore, crystal lattice analysis of compound **3** reveals an intermolecular hydrogen bond between the amide carbonyl of one molecule to the 7-hydroxyl group of another molecule, which may result in tight crystal lattice packing, that in turn likely contributes to **3** having a low aqueous solubility of 19 μg/mL. It was hypothesized that removal of the amide carbonyl from the hydantoin core could eliminate the intermolecular hydrogen bonding and thereby improve aqueous solubility to facilitate formulation work.

Table 1. Androgen Receptor Binding (K_i) and Functional (EC_{50}) Potency[a]

Compd	Structure[b]	R	K_i (nM)	EC_{50} (nM)
3	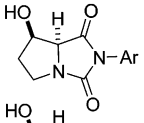		1.4	0.7
7			3.2	2.3
8	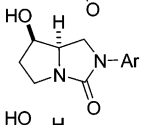		2.0	15
9	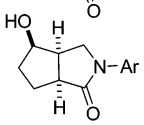		2.2	20
10a	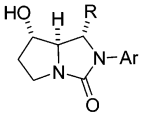	Me	1.5	5.2
11a		Et	0.9	1.8
12a		CF_3	0.9	2.5
10b	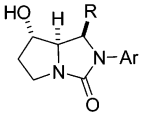	Me	4.0	87
11b		Et	1.6	7.1
12b		CF_3	1.9	48 (IA=65%)
10c	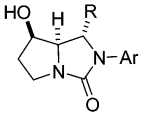	Me	2.9	13
11c		Et	0.7	2.6
12c		CF_3	1.0	2.9
11d	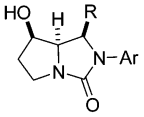	Et	2.3	7.4
12d		CF_3	2.2	2.1
13		*i*-Pr	23	108 (IA=75%)
14	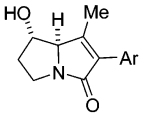		0.5	2.0

[a] In vitro data are at lease two separate measurements using DHT as a control in both AR binding ($K_i = 0.25 \pm 0.03$ nM) and functional agonist assay ($EC_{50} = 2.8 \pm 0.5$ nM). Unless otherwise noted, all compounds are full AR agonist (IA > 85%) relative to DHT control (IA = 100%). [b] Ar is 4-cyanonaphen-1-yl for compound **7**; 3-chloro-4-cyano-2-methylphen-1-yl for compounds **3**, **8**−**14**.

In Vitro Activity. Based on these rationales, the simple imidazolin-2-one **8** was first prepared as a baseline des-oxo analogue and was shown to be a fully efficacious AR agonist with an EC_{50} of 15 nM. This initial finding indicated that removal of the amide carbonyl of hydantoin ring was tolerated but that additional optimization to find a more suitable amide carbonyl replacement was needed in order to retain the AR functional potency of the parent molecule **3**. Our attention then turned to the alkyl-substituted imidazolin-2-ones such as compounds **10**−**13** (Figure 2) in order to investigate the feasibility of small hydrophobic groups as the more optimal surrogates for the amide carbonyl group. Methyl- and ethyl-substituted imidazolin-2-ones **10a**−**c** and **11a**−**d** were highly potent in the AR binding assay with K_is in the range of 0.9 to

4 nM, whereas the ethyl analogues **11a**−**c** demonstrated a 3 to 12-fold enhanced functional potency versus the corresponding methyl analogues **10a**−**c** (i.e., **11c**, EC_{50} = 2.6 nM vs **10c**, EC_{50} = 13.2 nM). Trifluoromethyl-substituted imidazolin-2-ones **12a**−**d** were also evaluated since the trifluoromethyl group was considered to be comparable in size to an ethyl group but might be more metabolically stable in vivo. In both AR binding and functional assays, compounds **12a**−**d** were found to have in vitro activity similar to that of ethyl analogues **11a**−**d**, confirming that the trifluoromethyl group can function as a suitable steric replacement with Van der Waals interactions to the neighboring residues in the binding pocket.

As was recently shown for the *N*-aryl hydroxybicyclohydantoin series, both the relative and absolute stereochemical configuration of the 7-hydroxyl and ring juncture 7*a*-hydrogen can have a significant impact on biological activity, particularly in the AR functional assay.[29] It is also noted that there is a slight preference for the *R*-configuration with respect to 7*a*-hydrogen. Four sets of imidazolin-2-one diastereomers, varying the 7-hydroxyl and 1-alkyl positions, were evaluated with 7*a*-hydrogen being fixed in the *R*-configuration (Figure 2). The effects of the 7-hydroxyl configuration for these alkyl-substituted imidazolin-2-ones **10**−**12** were found to have little impact on activity. This is most readily illustrated in the comparison of examples **10a**, **11a**, or **12a** versus **10c**, **11c**, or **12c**, respectively, where the potency difference between the pairs is generally within 2-fold (Table 1). On the other hand, there is a slight preference for the *S*-stereochemistry for 1-alkyl substitution. For example, compound **10a** (EC_{50} = 5.2 nM) is 16-fold more potent than **10b** (EC_{50} = 87 nM), and **11c** (EC_{50} = 2.6 nM) is 3-fold more potent than **11d** (EC_{50} = 7.4 nM). Size limitations at this position were also apparent, as the larger isopropyl group in imidazolin-2-one **13** resulted in a substantial loss of both AR binding and functional potency.

Carbon replacement of the ring juncture nitrogen in **8** was also assessed with corresponding pyrrolidinone **9**, which was found to exhibit comparable in vitro potency to that of compound **8**. Replacement of the sp^2 aniline nitrogen with an sp^2 carbon, as in pyrrol-2-one **14**, was also evaluated as a means of obviating metabolic release of an aniline, and compound **14** was a very potent AR agonist. However, because compound **14** slowly eliminated water under mildly acidic conditions to form an olefinated byproduct, no further optimization was attempted with the pyrrol-2-one scaffold.

In order to gain insight into the molecular interactions of these alkyl-substituted imidazolin-2-ones within the AR-LBD, molecular docking studies were conducted using **11a** as a probe. Much like those key interactions observed in the X-ray cocrystal structure of hydantoin **3**, the binding model of **11a** was also dominated by the interaction between the cyano group with the guanidinium moiety of Arg-752 to form a nonclassical hydrogen bond of 2.6 Å length (Figure 3b). However, unlike the case of **3**, the 7-hydroxyl group of **11a** appeared capable of forming a bifurcated hydrogen bond with both Asn-705 (3.0 Å) and Thr-877 (2.8 Å). A similar bifurcated hydrogen bond to both Asn-705 and Thr-877 was also observed in the endogenous steroid ligand DHT cocrystal structure.[40] The dihedral angle between the aryl and imidazolin-2-one ring of **11a** was determined to be 58°, likely inducing the aryl group into a favorable orientation for the π-edge-face interaction with the Phe-764 residue. The docking studies also suggested that replacing the amide carbonyl in **3** with small alkyl groups such as methyl, ethyl or trifluoromethyl, as in compounds **10**, **11**, or **12**, respectively, fit well in the hydrophobic pocket surrounded by Trp-741, Met-742, and Met-745. However, the larger isopropyl group in **13**, which leads to 10−15-fold reduced potency compared to **11** or **12** in the in vitro assay, exceeds the available space in the hydrophobic pocket and thus causes unfavorable helical deformation of the LBD.

A preliminary assessment of aqueous solubility was conducted for compounds **8** (245 μg/mL), **10a** (613 μg/mL), **11a** (242 μg/mL), and **12d** (1140 μg/mL) using crystalline or amorphous solid.[41] Despite the higher log *P* values for these imidazolin-2-ones, all showed an improvement in aqueous solubility compared with hydantoin **3** (19 μg/mL). These results are consistent with our initial hypothesis that removal of the amide carbonyl from the hydantoin core would eliminate intermolecular hydrogen bonding between 7-hydroxyl in one molecule to amide carbonyl group of another molecule in the crystal lattice, thus obviating the potential for tight crystal lattice packing. Accompanying these observations is the fact that the melting points for **8**, **10a**, **11a**, and **12d** are at least 50 °C lower than that of **3**, suggesting looser crystal packing as a likely reason for the improved aqueous solubility.[41]

In Vivo Pharmacological Evaluation. On the basis of in vitro pharmacological activity as well as data from a panel of pharmaceutical profiling assays (including Caco-2 permeability, CYP inhibition, liver microsomal stability, human hepatotocyte toxicity, hERG inhibition, etc.), compounds **8**, **9**, **10a**, **11a**, **12c**, and **12d** were selected for evaluation of their in vivo pharmacology. The compounds were assessed for efficacy and selectivity in the stimulation of muscle vs prostate tissue growth in castrated male rats, a pharmacological model that has been widely used for the assessment of anabolic and androgenic activities.[42,43] In this model, mature male rats were castrated two weeks prior to oral administration of test compounds. After an additional two weeks of treatment, both levator ani muscle and ventral prostate tissues were weighed and compared to those from a sham-operated, vehicle-treated control group. In addition, plasma concentrations of testing compounds were measured following a single 10 mg/kg oral dose to gain understanding of pharmacokinetic/pharmacodynamic relationships. As summarized in Table 2, compounds **8**, **9**, **10a**, and **12c** showed approximately 40−66% recovery of muscle weight with minimal effect on prostate tissue at a once-daily oral screening dose of 1 or 3 mg/kg. Conversely, a somewhat weaker response was observed for trifluoromethyl-substituted imidazolin-2-one **12d** (EC_{50} = 2.1 nM), which is likely due at least in part to its poor systemic exposure. In contrast, ethyl-substituted **11a** (EC_{50} = 1.8 nM) achieved maximum muscle recovery at a dose of 1 mg/kg. A subsequent full dose response study determined that **11a** had an ED_{50} of 0.09 mg/kg for levator ani muscle and an ED_{50} of approximate 4.6 mg/kg for prostate tissue which amounts to 50-fold selectivity favoring muscle (Figure 4).[44] For comparison, testosterone propionate exhibited only 2-fold muscle selectivity in this model when given subcutaneously.[29] Pharmacokinetic studies in rats with **11a** indicate that this compound has an oral bioavailability of 65% and a plasma half-life of 5.5 h.[45] Compound **11a** is selective versus other steroid hormone receptors (PR, ER_α, ER_β, GR), as well as for SHBG binding and aromatase inhibition, is clean in human hepatocyte toxicity assays, and has only weak inhibition of CYP450 isozymes and hERG (patch clamp).[46] Furthermore, compound **11a** is negative in an exploratory Ames genotoxicity assay.[47]

In summary, based on pharmacophore modeling studies which emerged from the cocrystal structure of our first generation SARM **3**, a systematic SAR exploration of the hydantoin scaffold was carried out to provide a novel series of imidazolin-

Table 2. In Vivo Evaluation of Muscle and Prostate Tissue Growth and Oral Exposure in Rats

			in vivo results		oral exposure at 10 mg/kg	
compd[a]	EC_{50} (nM)	dose (mg/kg)	muscle[b]	prostate[b]	C_{max} (nM)	$AUC_{(0-4h)}$ (nM·h)
3	0.7	0.01	59 ± 3	3 ± 1	6896	8797
8	15	1	66 ± 3	14 ± 4	3972	6378
9	20	1	45 ± 2	6 ± 1	ND[c]	ND[c]
10a	5.2	3	44 ± 2	4 ± 1	1625	2893
11a	1.8	1	101 ± 4	24 ± 3	3096	6078
12c	2.9	1	40 ± 2	3 ± 0	819	1182
12d	2.1	1	30 ± 1	1 ± 0	245	630
TP	2.8	0.3	70 ± 4	68 ± 5	ND[c]	ND[c]

[a] All compounds were administrated orally once a day at dose indicated. Testosterone propionate (TP) was dosed subcutaneously. A historical result of compound **3** was included for comparison; see ref 28 for details. [b] The percent weight of rat levator ani muscle or ventral prostate tissue compared to intact control group ± SEM (%). [c] Not determined.

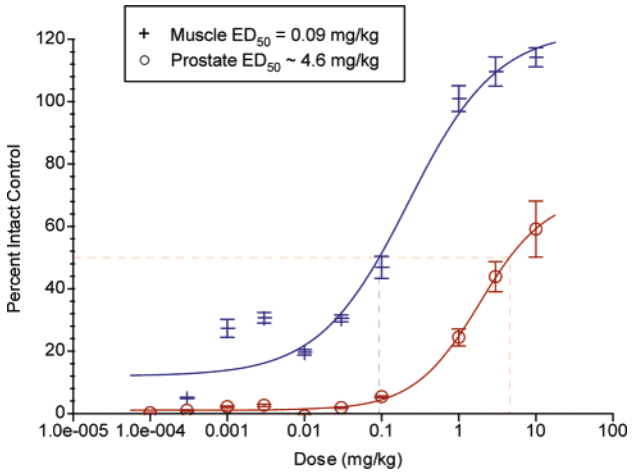

Figure 4. Effects of once daily treatment with compound **11a** on levator ani muscle and prostate tissue growth in a 14-day dose−response study.

2-ones **10**−**12** as highly potent and orally active AR agonists. The lead compound in the new series, **11a**, had a K_i of 0.9 nM and EC_{50} of 1.8 nM in the AR binding and functional assays, respectively, and exhibited 50-fold selectivity for muscle growth in a mature orchidectomized rat model. The overall pharmacological, ADME, and pharmaceutics profile of this potent SARM suggests that **11a** is a suitable SARM drug candidate for further development.

Experimental Section

General Chemistry Methods. Proton and carbon-13 NMR spectra were recorded on Jeol 400 MHz or 500 MHz instrument. Analytical HPLC was performed on a Shimadzu HPLC using YMC C18 5 μm 4.6 × 50 mm column with a 4 min gradient of 0−100% solvent A (90% MeOH/90% H_2O/0.2% H_3PO_4) and 100−0% of solvent B (10% MeOH/90% H_2O/0.2% H_3PO_4) with a 1 min hold. LC-MS spectra were obtained on a Shimadzu HPLC and Micromass Platform using electrospray ionization. HRMS were obtained on a Micromass LCT in lockspray with electrospray ionization. The preparative HPLC was done on an automated Shimadzu system using YMC ODS C18 5 micron preparative columns with mixtures of solvent C (90% MeOH/10% H_2O/0.2% TFA) and solvent D (10% MeOH/90% H_2O/0.2% TFA) or mixtures of solvent E (90% CH_3CN/10%H_2O/0.2% TFA) and solvent F (10% CH_3CN/90% H_2O/0.2% TFA). Melting point (°C) was measured on the Mel-Temp II device and was uncorrected. Preparation of intermediates **16**, **17a**, **17b**, **23**, and **25** are described in Supporting Information, and other reagents and solvent were obtained from commercial sources and were used without further purification. All reactions were carried out under a nitrogen atmosphere unless otherwise noted.

(7*R*,7a*R*)-2-Chloro-4-(7-hydroxy-3-oxotetrahydropyrrolo[1,2-*c*]imidazol-2-yl)3-methylbenzonitrile (8). To a solution of **3** (150 mg, 0.5 mmol) in anhydrous THF (12 mL) was added $LiEt_3BH$ (0.5 mL, 0.5 mmol, 1.0 M in THF) at −78 °C. The reaction was stirred at −78 °C for 4 h and then quenched with a saturated aqueous solution of Na_2CO_3 (5 mL). The reaction mixture was allowed to warm to 0 °C, a solution of 30% H_2O_2 (∼ 0.5 mL) was added, and the stirring was continued at 0 °C for another 30 min before being extracted with CH_2Cl_2 (3×). The combined extracts were washed with brine, dried (Na_2SO_4), and concentrated. The residue (120 mg) was dissolved in anhydrous CH_2Cl_2, and triethylsilane (0.5 mL, 3.1 mmol) was added at −78 °C followed by BF_3Et_2O (0.5 mL, 3.9 mmol). After the mixture was stirred at −78 °C for 2 h, additional triethylsilane (0.3 mL, 1.88 mmol) and BF_3Et_2O (0.3 mL, 2.35 mmol) were added, and the stirring was continued at 0 °C overnight. The reaction was quenched with a saturated aqueous solution of Na_2CO_3 (10 mL), and extracted with CH_2Cl_2 (3×). The combined extracts were washed with brine, dried (Na_2SO_4), and concentrated. Purification by reverse phase preparative HPLC followed by chiral preparative HPLC (Chiralpak OD, 20% IPA in hexanes) afforded **8** (9 mg, 6%). HPLC: 98%; ^{1}H NMR (CD_3OD) δ 2.04−2.13 (m, 2 H), 2.34 (s, 3 H), 3.22 (ddd, J = 10.8, 9.0, 3.1 Hz, 1 H), 3.64 (ddd, J = 10.0, 10.0, 8.6 Hz, 1 H), 3.90 (d, J = 2.6 Hz, 1 H), 3.91 (s, 1 H), 3.99−4.03 (m, 1 H), 4.16−4.19 (m, 1 H), 7.39 (d, J = 8.3 Hz, 1 H), 7.66 (d, J = 8.3 Hz, 1 H); LC-MS m/z 292 $[M+H]^+$; HRMS calcd for (M+H) 292.0843, found 292.0843.

2-Chloro-4-((3a*R*,4*R*,6a*S*)-4-hydroxy-1-oxo-hexahydrocyclopenta[*c*]pyrrol-2(1*H*)-yl)-3-methylbenzonitrile (9). Step 1. *N*-Arylation. To a vial containing compound **15**[37] (100 mg, 0.4 mmol) in dioxane (1 mL) were added CuI (15.6 mg, 0.08 mmol), K_3PO_4 (174 mg, 0.82 mmol), 1,2-cyclohexyldiamine (4.7 mg, 0.08 mmol), and **16** (136 mg, 0.49 mmol). The vial was sealed, heated at 110 °C for 14 h, and cooled to room temperature. The solid was filtered and the filtrate concentrated. Purification by silica gel chromatography (eluting with 5−100% EtOAc in hexanes and then 10% MeOH in EtOAc), followed by chiral preparative HPLC (Chiralpak AD, 20% IPA in heptane and then Chiralpak OD, 6% MeOH and 6% EtOH in heptane) provided *N*-arylated benzoyl ester (24 mg, 21%). ^{1}H NMR (CD_3OD) δ 1.94−2.00 (m, 1H), 2.03−2.18 (m, 3 H), 2.20 (s, 3 H), 3.25−3.35 (m, 2H), 3.72 (d, J = 9.9 Hz, 1H), 3.80 (dd, J = 2.2, 8.2 Hz, 1H), 5.50 (q, J = 6.0 Hz, 1H), 7.20 (d, J = 8.2 Hz, 1H), 7.41 (t, J = 7.7 Hz, 2H), 7.52 (d, J = 8.2 Hz, 1H), 7.56 (t, J = 7.7 Hz, 1H), 7.92 (d, J = 7.7 Hz, 2H); LC/MS (m/z) 395 $[M+H]^+$.

Step 2. Hydrolysis of Benzoyl Ester. To a stirred solution of benzoyl ester obtained from step 1 (24 mg, 0.06 mmol) in THF (2 mL) was added KOH (0.09 mL, 1 M in MeOH) at 0 °C, and the stirring was continued at 0 °C for 3 h. The reaction was quenched with 1 N HCl (0.09 mL) and diluted with EtOAc and water. The organic layer was separated, washed with water, dried (Na_2SO_4), and concentrated. Purification by silica gel chromatography, eluting with 5−80% EtOAc in hexanes, provided **9** (15 mg, 88%). ^{1}H NMR ($CDCl_3$) δ 1.73 (ddd, J = 12.9, 12.9, 6.6 Hz, 1H), 1.91 (ddd, J = 20.5, 7.3, 4.7 Hz, 1H), 2.00−2.10 (m, 1H), 2.11−2.20 (m, 1H), 2.29 (s, 3 H), 2.85−2.92 (m, 1H), 3.14 (ddd, J = 9.6, 9.6, 4.4 Hz, 1H), 3.90 (dd, J = 9.9, 2.2 Hz, 1H), 4.41 (q, J = 5.5 Hz, 1H), 7.22

(d, J = 8.2 Hz, 1H), 7.52 (d, J = 8.2 Hz, 1H); LC-MS m/z 291 $[M+H]^+$; HRMS calcd for [M+H] 291.0900, found 290.0897; $[\alpha]_D$ = +80.7° (589 nm, c = 0.091 w/v% in MeOH); Anal. ($C_{15}H_{15}ClN_2O_2$) C, H, N.

2-Chloro-4-((1*S*,7*S*,7a*R*)-1-ethyl-7-hydroxy-3-oxo-tetrahydro-1*H*-pyrrolo[1,2-*e*]imidazol-2(3*H*)-yl)-3-methylbenzonitrile (11a) is described as a typical procedure for **10a**, **10b**, and **11b** (Scheme 2).

Step 1. Alcohols **18a** (R = Et) and **18b** (R = Et). To a stirred solution of aldehyde **17a** (13.0 g, 39.5 mmol) in anhydrous THF (100 mL) was added dropwise EtMgBr (79.0 mL, 79.0 mmol, 1.0 M in THF) under nitrogen, and the temperature was kept below −60 °C during the addition. The reaction was stirred at 0 °C for 2 h and then quenched with HOAc (4.5 mL, 79 mmol) at 0 °C. The mixture was concentrated and then diluted with EtOAc. The organic layer was washed with brine, dried (Na_2SO_4), and concentrated. Purification by silica gel chromatography, eluting with 10% EtOAc in hexanes, provided **18a** (4.1 g, 29%; first eluting isomer) and **18b** (4.0 g, 28%; second eluting isomer), both as oils. Alcohol **18a**. ^{1}H NMR ($CDCl_3$) δ 0.05 and 0.06 (s, total 6H), 0.85 and 0.86 (s, total 9H), 1.01 (t, J = 7.3 Hz, 3H), 1.46 (s, 9H), 1.52−1.65 (m, 2H), 1.68−1.80 (m, 1H), 1.85−2.05 (m, 1H), 3.20−3.40 (m, 1H), 3.45−3.62 (m, 1H), 3.64−3.73 (m, 1H), 4.07−4.14 (m, 1H).

Step 2. Ketone **19** (R = Et). To the mixtures of **18a** and **18b** (1.9 g, 5.3 mmol) in 50 mL of CH_3CN and CH_2Cl_2 (1:9) at room temperature was added 4-methyl morpholine *N*-oxide (1.50 g, 12.8 mmol), followed by tetrapropylammonium perruthenate (95 mg, 0.27 mmol). The reaction was stirred at room temperature for 2 h and then diluted with hexanes (50 mL). The mixture was filtered through a pad of silica gel and concentrated. Purification by silica gel chromatography, eluting with 10% EtOAc in hexanes, provided ketone **19** (1.66 g, 87%) as an oil. ^{1}H NMR ($CDCl_3$) δ 0.06 and 0.07 (s, total 6H), 0.86 (s, 9H), 1.04 and 1.05 (t, J = 7.1 Hz, total 3H), 1.74−1.79 (m, 1H), 1.88−1.93 (m, 1H), 2.49 and 2.57 (q, J = 8.0 Hz, total 2H), 3.46−3.64 (m, 2H), 4.09 and 4.23 (d, J = 2.8 Hz, total 2H), 4.17−4.21 (m, 1H).

Step 3. Oxime Intermediate. To a solution of ketone **19** (1.66 g, 4.6 mmol) in MeOH (15 mL) were added NH_2OH HCl (960 mg, 13.8 mmol) and NaOAc (1.13 g, 13.8 mmol) at room temperature. The suspension was stirred at room temperature for 2 h, filtered, washed with EtOAc, and concentrated. Purification by silica gel chromatography, eluting with 10% EtOAc in hexanes, provided the oxime intermediate (1.7 g, 100%) as an oil. ^{1}H NMR ($CDCl_3$) δ 0.06 and 0.07 (s, total 6H), 0.86 and 0.87 (s, total 9H), 0.99−1.20 (m, total 3H), 1.42 and 1.46 (s, total 9H), 1.68−1.85 (m, 1H), 1.96−2.08 (m, 1H), 2.10−2.31 (m, 1H), 2.39−2.54 (m, 1H), 3.39−3.70 (m, 2H), 4.12 and 4.23 (s, total 1H).

Step 4. Amine **20a** (R = Et). To a 100 mL pressure reaction vessel containing oxime (1.7 g, 4.6 mmol) from the previous step in MeOH (40 mL) were added a slurry of Raney Ni (ca. 4.3 g, in water), 10% Pd/C (200 mg, Degussa type), ammonia in MeOH (2.0 M, 10 mL), and water (2 mL). The vessel was carefully evacuated under vacuum until the solvent bubbled gently. Hydrogenation (80 psi H_2) was carried out at room temperature overnight. The catalyst was removed by filtration, washed with additional MeOH, and concentrated. Purification by silica gel chromatography, eluting with 5−20% MeOH in CH_2Cl_2, provided **20a** (1.55 g, 95%) as an oil. ^{1}H NMR ($CDCl_3$) δ 0.05 (s, 6H), 0.85 (s, 9H), 1.00 (br s, 3H), 1.45 (s, 9H), 1.85−2.05 (m, 4H), 2.30−2.55 (m, 1H), 3.34 (br s, 1H), 3.24−3.73 (m, 3H), 4.11 (br s, 1H).

Step 5. Aniline **21** (R = Et). To a solution of amine **20a** (600.0 mg, 1.7 mmol) in anhydrous toluene (7 mL) were added **16** (700 mg, 2.5 mmol), $Pd_2(dba)_3$ (154 mg, 0.17 mmol), (*R*)-*N*,*N*-dimethyl-1-[(*R*)-2-(diphenyphosphino)ferrocenyl]ethylamine (225 mg, 0.51 mmol), Cs_2CO_3 (850 mg, 3.4 mmol), and DMSO (1 mL) at room temperature. After the solution was degassed with N_2 for 10 min, the reaction mixture was heated at 100 °C for 48 h and then cooled to room temperature. The reaction was diluted with EtOAc (50 mL), washed with water, dried (Na_2SO_4), filtered, and concentrated. Purification by silica gel chromatography, eluting with 0−10% EtOAc in hexanes, provided **21** (177 mg, 21%) as an oil. ^{1}H NMR ($CDCl_3$) δ 0.05 (s, 6H), 0.84 (s, 9H), 0.94 (t, J = 7.5 Hz, 3H), 1.41 (s, 9H), 1.78−1.89 (m, 2H), 1.91−2.01 (m, 1H), 2.21 (s, 3H), 3.17−3.31 (m, 3H), 3.43−3.58 (m, 1H), 3.90 (d, J = 9.7 Hz, 1H), 4.19 (J = 2.6 Hz, 1H), 5.53 (d, J = 4.8 Hz, 1H), 6.38 (d, J = 8.4 Hz, 1H), 7.31 (d, J = 8.4 Hz, 1H); LC-MS m/z 508 $[M+H]^+$.

Step 6. Boc Deprotection and Cyclization. Aniline **21** (177 mg, 0.35 mmol) was dissolved in 15% TFA/CH_2Cl_2 (8 mL) and stirred at room temperature for 3 h. The reaction was quenched with 1 N NaOH and diluted with CH_2Cl_2. The organic layer was washed with water, dried (Na_2SO_4), and concentrated. The residue was dissolved in THF (3 mL) and cooled to 0 °C. *i*-Pr_2NEt (183 μL, 1.00 mmol) was added followed by a phosgene solution (220 μL, 0.42 mmol, 1.9 M in toluene), and the stirring was continued for 10 min at 0 °C and then room temperature for 60 min before being quenched with water. The mixture was concentrated, diluted with EtOAc, washed with water, dried (Na_2SO_4), and concentrated. Purification by silica gel chromatography, eluting with 10−30% EtOAc in hexanes, provided TBS-protected **11a** (130 mg, 86%) as a solid. ^{1}H NMR ($CDCl_3$) δ 0.10 (s, 6H), 0.88 (t, J = 7.0 Hz, 3H), 0.90 (s, 9H), 1.46−1.55 (m, 1H), 1.86 (dddd, J = 12.8, 8.8, 8.6, 8.4 Hz, 1H), 2.18 (dddd, J = 12.1, 8.2, 7.9, 4.2 Hz, 1H), 2.30 (s, 3H), 3.34 (ddd, J = 13.2, 9.7, 4.0 Hz, 1H), 3.40 (dd, J = 6.8, 2.9 Hz, 1H), 3.67 (ddd, J = 11.9, 8.4, 8.4 Hz, 1H), 3.90 (br s, 1H), 4.00 (q, J = 7.5 Hz, 1H), 7.11 (br s, 1H), 7.52 (d, J = 8.3 Hz, 1H); LC-MS m/z 435 $[M+H]^+$.

Step 7. Compound **11a**. To a solution of TBS-protected **11a** (130 mg, 0.3 mmol) from previous step in THF (2 mL) was added Bu_4NF (0.7 mL, 0.7 mmol, 1.0 M in THF), and the reaction was stirred at room temperature for 60 min. The reaction was quenched with water and then concentrated. The residue was diluted with EtOAc, washed with water, dried (Na_2SO_4), and concentrated. Purification by silica gel chromatography, eluting with 50−100% EtOAc in hexanes, followed by reverse phase preparative HPLC (YMC S5 ODS-A 30 × 75 mm C18 column) provided **11a** (65 mg, 68%) as a white solid. ^{1}H NMR ($CDCl_3$) δ 0.90 (t, J = 7.4 Hz, 3H), 1.46−1.66 (m, 2H), 1.90 (dddd, J = 14.0, 7.1, 7.1, 6.9 Hz, 1H), 2.24 (dddd, J = 13.0, 8.0, 6.5, 6.3 Hz, 1H), 2.30 (s, 3H), 3.34 (ddd, J = 14.0, 8.6, 5.1 Hz, 1H), 3.46 (dd, J = 5.9, 5.6 Hz, 1H), 3.72 (ddd, J = 15.1, 7.9, 7.9 Hz, 1H), 4.01 (t, J = 2.8 Hz, 1H), 4.13 (q, J = 6.9 Hz, 1H), 7.12 (d, J = 7.9 Hz, 1H), 7.51 (d, J = 8.2 Hz, 1H); ^{13}C NMR ($CDCl_3$) δ 8.7, 16.3, 26,1, 34.3, 43.9, 62.9, 67.7, 75.6, 111.6, 116.2, 123.2, 131.2, 136.6, 138.4, 142.0, 160.0; LC-MS m/z 320 $[M+H]^+$; HRMS calcd for $(M-H)^-$ 318.1009, found 318.0994; $[\alpha]_D$ = −92.3 (c = 0.6667 w/v% in MeOH, 23.9 °C); Anal. ($C_{16}H_{18}ClN_3O_2 \cdot 0.7 H_2O$) C, H, N.

(2*R*,3*S*)-*N*-*tert*-Butyloxycarbonyl-3-(*tert*-butyldimethylsilanyloxy)-2-((1*R*)-1-aminopropyl)pyrrolidine (20b, R = Et). Step 1. Mesylate formation. To a solution of alcohol **18a** (1.25 g, 3.5 mmol) in CH_2Cl_2 (20 mL) were added *i*-Pr_2NEt (2.44 mL, 14.0 mmol) and DMAP (21 mg, 0.17 mmol) at room temperature, and the mixture was cooled to 0 °C. CH_3SO_2Cl (0.54 mL, 6.9 mmol) was added at 0 °C, and the reaction was stirred at 0 °C for 20 min followed by room temperature for 3 h. The reaction was quenched with water and then concentrated. The residue was diluted with EtOAc, washed with water, dried (Na_2SO_4) and concentrated. Purification by silica gel chromatography, eluting with 10% EtOAc in hexanes, provided mesylate intermediate (1.20 g, 78%) as a colorless oil. ^{1}H NMR ($CDCl_3$) δ 0.06 (s, 3H), 0.07 (s, 3H), 0.85 (s, 9 H), 1.03 (t, J = 7.3 Hz, 3H), 1.44 and 1.47 (s, total 9 H), 1.58−1.73 (m, 1H), 1.73−1.88 (m, 1H), 1.89−2.02 (m, 1H), 2.99 and 3.04 (s, total 3H), 3.52 and 3.62 (ddd, J = 9.8, 9.8, 7.7 Hz, total 1H), 3.85−3.98 (m, 1H), 4.23−4.32 (m, 1H), 4.57−4.80 (m, 1H).

Step 2. Sodium Azide Displacement. To a solution of the above mesylate intermediate (1.20 g, 2.74 mmol) in DMF (20 mL) was added NaN_3 (890 mg, 13.7 mmol), and the reaction was heated at 80 °C overnight. The reaction was quenched with water and then concentrated. The residue was diluted with EtOAc, washed with water, dried (Na_2SO_4), and concentrated. Purification by silica gel chromatography, eluting with 10% EtOAc in hexanes, provided the azide intermediate (810 mg, 77%) as a colorless oil. ^{1}H NMR

($CDCl_3$) δ 0.04 (s, 6 H), 0.84 (s, 9 H), 1.03 (t, J = 7.3 Hz, 3H), 1.45 and 1.55 (s, total 9 H), 1.50−1.61 (m, 1H), 1.67−1.80 (m, 1H), 2.03−2.15 (m, 1H), 3.30−3.44 (m, 1H), 3.44−3.55 (m, 1H), 3.55−3.66 (m, 1H), 3.66−3.71 (m, 1H), 3.87−3.96 (m, 1H), 4.21−4.31 (m, 1H); LC-MS m/z 385 $[M+H]^+$.

Step 3. Amine **20b** (R = Et). To a solution of the above azide intermediate (810 mg, 2.1 mmol) in MeOH (15 mL) was added 10% Pd−C (160 mg, 5% dry basis), and the reaction was stirred under a H_2 balloon for 3 h. The catalyst was removed by filtration, washed with MeOH, and concentrated to give **20b** (740 mg, 98%) as a colorless oil. ^{1}H NMR ($CDCl_3$) δ 0.04 (s, 3H), 0.05 (s, 3H), 0.84 (s, 9 H), 0.96 (t, J = 7.3 Hz, 3H), 1.15−1.36 (m, 2H), 1.49−1.63 (m, 1H), 1.73 (br s, 1H), 2.02 (dddd, J = 13.1, 8.7, 8.7, 4.6 Hz, 1H), 2.90 and 3.09 (br s, total 1H), 3.32 (t, J = 7.9 Hz, 1H), 3.49 (br s, 1H), 3.61 (br s, 1H), 4.34 (br s, 1H); LC-MS m/z 359 $[M+H]^+$.

2-Chloro-4-((1*S*,7*S*,7a*R*)-7-hydroxy1-methyl-3-oxo-tetrahydro-1*H*-pyrrolo[1,2-*e*]imidazol-2(3*H*)-yl)-3-methylbenzonitrile (10a) is prepared using amine **20a** (R = Me). ^{1}H NMR (CD_3OD, 400 MHz) δ 1.25 (d, J = 6.6 Hz, 3H), 1.82−1.92 (m, 1H), 2.15−2.25 (m, 1H), 2.30 (s, 3H), 3.39 (s, 1H), 3.54−2.65 (m, 1H), 4.13 (q, J = 6.6 Hz, 1H), 4.33 (bs, 1H), 7.35 (d, J = 8.3 Hz, 1H), 7.69 (d, J = 8.3 Hz, 1H); ^{13}C NMR (CD_3OD, 125 MHz) δ 16.2, 19.9, 34.7, 44.8, 71.7, 75.7, 116.8, 132.7, 137.9, 138.5, 143.1; LC-MS m/z 306 $[M+H]^+$; HRMS calcd for [M+H] 306.1009, found 306.1002; Anal. ($C_{15}H_{16}ClN_3O_2 \cdot 0.1\ H_2O$) C, H, N.

2-Chloro-4-((1*R*,7*S*,7a*R*)-7-hydroxy1-methyl-3-oxo-tetrahydro-1*H*-pyrrolo[1,2-*e*]imidazol-2(3*H*)-yl)-3-methylbenzonitrile (10b) is prepared using amine **20b** (R = Me). HPLC purity: 98%; ^{1}H NMR (CD_3OD) δ 1.23 (d, J = 6.6 Hz, 3H), 1.79−1.92 (m, 1H), 2.23−2.35 (m, 1H), 2.31 (s, 3H), 3.26−3.35 (m, 1H), 3.55−3.70 (m, 2H), 4.09 and 4.24 (q, J = 7.9 Hz, total 1H), 4.47 (br s, 1H), 7.37 (d, J = 8.3 Hz, 1H), 7.71 (d, J = 8.3 Hz, 1H); LC-MS m/z 306 $[M+H]^+$; HRMS calcd for [M+H] 306.1009, found 306.1010.

2-Chloro-4-((1*R*,7*S*,7a*R*)-1-ethyl-7-hydroxy-3-oxo-tetrahydro-1*H*-pyrrolo[1, 2-*e*]imidazol-2(3*H*)-yl)-3-methylbenzonitrile (11b) is prepared using amine **20b** (R = Et). ^{1}H NMR ($CDCl_3$) δ 0.96 (t, J = 7.5 Hz, 3H), 1.45−1.57 (dddd, J = 21.3, 7.7, 7.7, 4.2 Hz, 1H), 1.68 (dddd, J = 20.8, 10.2, 7.1, 7.1 Hz, 1H), 1.78−1.89 (m, 1H), 2.24−2.34 (m, 1H), 2.28 (s, 3H), 3.29 (ddd, J = 12.0, 9.4, 5.1 Hz, 1H), 3.71 (t, J = 7.5 Hz, 1H), 3.76 (ddd, J = 12.1, 8.8, 6.6 Hz, 1H), 4.08 (br s, 1H), 4.32 (q, J = 7.5 Hz, 1H), 7.11 and 7.15 (d, J = 8.2 Hz, total 1H), 7.53 (d, J = 8.2 Hz, 1H); LC-MS m/z 320 $[M+H]^+$; HRMS calcd for [M+H] 320.1166, found 320.1152; Anal. ($C_{16}H_{18}ClN_3O_2$) C, H, N.

2-Chloro-4-((1*S*,7*R*,7a*R*)-1-ethyl-7-hydroxy-3-oxo-tetrahydro-1*H*-pyrrolo[1, 2-*e*]imidazol-2(3*H*)-yl)-3-methylbenzonitrile (11c) is described as a typical procedure for **10c** and **11d**. Step 1. Mitsunobu Reaction. To a solution of compound **11a** (51 mg, 0.16 mmol) in THF (2 mL) were added PPh_3 (84 mg, 0.32 mmol) and benzoic acid (39 mg, 0.32 mmol) followed by diisopropyl azodicarboxylate (65 mg, 0.32 mmol), and the mixture was stirred at room temperature for 2 h. The reaction was concentrated and then diluted with EtOAc. The organic layer was washed with water, dried (Na_2SO_4) and concentrated. Purification by silica gel column chromatography, eluting with 5−50% EtOAc in hexanes, yielded the benzoyl ester (64 mg, 94%) as a solid. ^{1}H NMR ($CDCl_3$) δ 0.87 (t, J = 7.5 Hz, 3H), 1.55−1.64 (m, 2H), 2.27 (br s, 3H), 2.25−2.34 (m, 2H), 3.36 (ddd, J = 11.6, 8.1, 3.5 Hz, 1H), 3.77 (t, J = 2.9 Hz, 1H), 3.85 (ddd, J = 11.1, 8.8, 8.8 Hz, 1H), 4.14 (ddd, J = 5.9, 5.9, 2.4 Hz, 1H), 5.59−5.65 (m, 1H), 6.81 (br s, 1H), 7.18−7.25 (m, 1H), 7.38 (t, J = 7.8 Hz, 2H), 7.58 (t, J = 7.6 Hz, 1H), 7.91 (dd, J = 8.3, 1.3 Hz, 2H).

Step 2. Benzoyl ester (64 mg, 0.15 mmol) from the previous step was dissolved in THF (1.5 mL) and then treated with KOH (0.32 mL, 0.32 mmol, 1 N in MeOH) at room temperature for 2 h. The reaction mixture with diluted with water and EtOAc. The organic layer was washed with saturated $NaHCO_3$ solution and brine, dried ($MgSO_4$), filtered, and concentrated. Purification by reverse phase preparative HPLC (Phenominex Luna 30 × 250 mm S5 C18 column) provided **11c** (43 mg, 88%) as a while solid. ^{1}H NMR (CD_3OD) δ 0.89 (t, J = 7.5 Hz, 3H), 1.60 (br s, 2H), 1.99−2.20 (m, 2H), 2.34 (s, 3H), 3.20 (ddd, J = 10.0, 10.0, 1.5 Hz, 1H), 3.54−3.68 (m, 2H), 4.18 (t, J = 2.9 Hz, 1H), 4.41 (br s, 4H), 7.38 (d, J = 7.5 Hz, 1H), 7.66 (d, J = 8.3 Hz, 1H); LC-MS m/z 320 $[M+H]^+$; HRMS calcd for [M+H] 320.1166, found 320.1152; Anal. ($C_{16}H_{18}ClN_3O_2$) C, H, N.

2-Chloro-4-((1*S*,7*R*,7a*R*)-7-hydroxy-1-methyl-3-oxo-tetrahydro-1*H*-pyrrolo[1,2-*e*]imidazol-2(3*H*)-yl)-3-methylbenzonitrile (10c). ^{1}H NMR (CD_3OD, 400 MHz) δ 1.24 (d, J = 6.2 Hz, 3H), 1.99−2.20 (m, 2H), 2.33 (s, 3H), 3.15−3.25 (m ,1H), 3.55 (t, J = 2.4 Hz, 1H), 3.62 (q, J = 9.4 Hz, 1H), 4.22 (s, 1H), 4.49 (bs, 1H), 7.36 (d, J = 7.9 Hz, 1H), 7.67 (d, J = 8.4 Hz, 1H); LC-MS m/z 306 $[M+H]^+$; HRMS calcd for $[M+H]^+$ 306.1009, found 306.1011; Anal. ($C_{15}H_{16}ClN_3O_2 \cdot 0.1\ H_2O$) C, H, N.

2-Chloro-4-((1*R*,7*R*,7a*R*)-1-ethyl-7-hydroxy-3-oxo-tetrahydro-1*H*-pyrrolo[1,2-*e*]imidazol-2(3*H*)-yl)-3-methylbenzonitrile (11d). HPLC purity: 97%; ^{1}H NMR ($DMSO_6$) δ 0.88 (t, J = 7.4 Hz, 3H), 1.29−1.42 (m, 1H), 1.82−1.92 (m, 2H), 1.92−2.06 (m, 1H), 2.27 (s, 3H), 3.05 (ddd, J = 10.9, 8.1, 3.0 Hz, 1H), 3.52−3.56 (m, J = 9.3 Hz, 1H), 3.61 (d, J = 7.7 Hz, 1H), 4.24−4.29 (m, 1H), 4.35 (t, J = 10.2 Hz, 1H), 4.83 (br s, 1H), 7.18 and 7.46 (d, J = 7.7 Hz, total 1H), 7.79 (d, J = 8.2 Hz, 1H), 7.82 (d, J = 8.2 Hz, 1H); LC-MS m/z 320 $[M+H]^+$, HRMS calcd for [M+H] 320.1166, found 320.1168.

2-Chloro-4-((1*S*,7*R*,7a*R*)-7-hydroxy-3-oxo-1-(trifluoromethyl)-tetrahydro-1*H*-pyrrolo[1,2-*e*]imidazol-2(3*H*)-yl)-3-methylbenzonitrile (12d) is described as a typical procedure for **12a**, **12b**, **12c**, and **13** (Schemes 3).

Step 1. Alcohols **22a** and **22b**. To aldehyde **17b** (2.10 g, 6.38 mmol) were added trimethyl(trifluoromethyl)silane (0.80 mL, 6.6 mmol) and CsF (10.0 mg, 0.066 mmol, dried under high vacuum at 130 °C for 12 h). The reaction was stirred at room temperature for 24 h and then heated at 50 °C for 5 h. After cooling to room temperature, an aqueous HCl solution (10 mL, 40 mmol, 4 N) was added, and the mixture was stirred overnight. The aqueous layer was decanted and the remaining waxy yellow solid was dried under high vacuum overnight and then recrystallized from hexanes to provide **22a** (1.19 g) as a white solid. The mother liquor was concentrated and purified by silica gel chromatography eluting with 5−20% EtOAc in hexanes to provide additional **22a** (100 mg, total 51%) and **22b** (192 mg, 8%) as an oil. Alcohol **22a**. ^{1}H NMR (CD_3OD) δ 0.12 (s, 3 H), 0.16 (s, 3 H), 0.92 (s, 9 H), 2.07−2.18 (m, 1H), 2.26 (dddd, J = 13.7, 9.9, 9.9, 3.8 Hz, 1H), 3.32−3.48 (m, 2H), 3.73 (dd, J = 8.5, 3.0 Hz, 1H), 4.44 (ddd, J = 14.8, 6.6, 6.6 Hz, 1H), 4.57 (br s, 1H).

Step 2. Urea **24a**. To alcohol **22a** (1.29 g, 3.23 mmol) in CH_2Cl_2 (24 mL) was added TFA (8 mL). After stirring for 30 min at room temperature, toluene (ca. 5 mL) was added, the reaction was concentrated, and the brown oil residue was dried under high vacuum overnight. The resulting Boc-deprotected intermediate was dissolved in CH_2Cl_2 (32 mL) and cooled to −78 °C. *i*-Pr_2NEt (1.13 mL, 6.49 mmol) was added, and the mixture was stirred for 15 min at −78 °C. Isocyanate **23** (621 mg, 3.23 mmol) in CH_2Cl_2 (5 mL) was added, and the reaction was allowed to warm to room temperature and stirred for 2 h. The reaction was quenched with water and then diluted with CH_2Cl_2. The organic layer was washed with brine, dried ($MgSO_4$), filtered, and concentrated. Purification by silica gel chromatography, eluting with 30−75% EtOAc in hexanes, provided **24a** (1.47 g, 93%) as a white solid. ^{1}H NMR ($CDCl_3$) δ 0.08 (s, 3 H), 0.10 (s, 3H), 0.89 (s, 9 H), 1.98−2.06 (m, 2H), 2.21 (s, 3 H), 3.49−3.58 (m, 1H), 3.72−3.83 (m, 1H), 3.92 (br s, 1H), 4.26 (t, J = 6.4, Hz, 1H), 4.46−4.55 (m, 2H), 7.12 (br s, 1H), 7.42 (d, J = 8.8 Hz, 1H), 7.84 (d, J = 8.8 Hz, 1H); LC-MS: m/z 492 $[M+H]^+$.

Step 3. Cyclization. To urea **24a** (1.44 g, 2.93 mmol) in THF (49 mL) at 0 °C was added *tert*-BuOK (8 mL, 8 mmol, 1 M in THF) followed by *p*-toluenesulfonyl chloride (720 mg, 3.8 mmol) in THF (5 mL). The cold bath was removed, and the reaction was stirred at room temperature for 90 min and then heated at 60 °C for 4 h. The reaction was quenched with water and then diluted with EtOAc. The aqueous layer was acidified to pH 1 with 1 N

HCl and extracted with EtOAc. The combined organics were washed with brine, dried ($MgSO_4$), filtered, and concentrated. Purification by silica gel chromatography, eluting with 30−75% EtOAc in hexanes, provided TBS-protected **12d** (956 mg, 69%) as a yellow foam. ^{1}H NMR ($CDCl_3$) δ 0.06 and 0.08 (s, total 3 H), 0.12 (s, 3 H), 0.89 (s, 9 H), 1.86−2.17 (m, 2H), 2.29 and 2.40 (s, total 3 H), 3.23−3.34 (m, 1H), 3.72 (ddd, J = 10.4, 10.4, 7.7 Hz, 1H), 3.84 and 3.89 (dd, J = 9.2, 1.8 Hz, total 1H), 4.54 and 4.85 (ddd, J = 16.9, 7.7, 7.5 Hz, 1H), 7.16 and 7.28 (d, J = 8.8 Hz, total 1H), 7.52 (d, J = 8.3 Hz, 1H); LC-MS: m/z 474 $[M+H]^+$.

Step 4. Compound **12d**. To TBS-protected **12d** (956 mg, 2.0 mmol) in THF (20 mL) was added Bu_4NF (2.5 mL, 2.5 mmol, 1 M in THF), and the reaction was stirred at room temperature for 2 h, quenched with saturated aqueous NH_4Cl, and then diluted with EtOAc. The organic layer was washed with brine, dried ($MgSO_4$), filtered, and concentrated. Purification by reverse phase preparative HPLC (YMC ODS C-18, 30 × 250 mm, eluting) provided **12d** (617 mg, 86%) as a white solid. ^{1}H NMR (CD_3OD) δ 1.98−2.12 (m, 1H), 2.34 and 2.39 (s, total 3H), 3.24 (ddd, J = 10.8, 8.0, 3.2 Hz, 1H), 3.62 and 3.71 (ddd, J = 10.0, 10.0, 8.8 Hz, total 1H), 3.97 and 4.03 (dd, J = 8.9, 2.0 Hz, total 1H), 4.39 (br s, 1H), 4.96 and 5.29 (ddd, J = 16.5, 8.2, 8.0 Hz, total 1H), 7.30 and 7.48 (d, J = 8.4 Hz, total 1H), 7.69 (d, J = 8.4 Hz, 1H); LC-MS: m/z 360 $[M+H]^+$; HRMS calcd for $(M+H)^+$ 360.0727, found 360.0738; Anal. ($C_{15}H_{13}ClF_3N_3O_2$) C, H, N, Cl.

2-Chloro-4-((1*R*,7*S*,7a*R*)-7-hydroxy-3-oxo-1-(trifluoromethyl)-tetrahydro-1*H*-pyrrolo[1,2-*e*]imidazol-2(3*H*)-yl)-3-methylbenzonitrile (12a). ^{1}H NMR (CD_3OD) δ 1.86−1.96 (m, 1H), 2.26 (ddd, J = 16.4, 8.4, 3.7 Hz, 1H), 2.31 and 2.35 (s, total 3H), 3.32−3.40 (m, 1H), 3.63 and 3.67 (dd, J = 7.1, 2.5 Hz, total 1H), 4.20 (q, J = 7.3 Hz, 1H), 5.04−5.11 (m, 1H), 7.33 and 7.49 (d, J = 8.7 Hz, total 1H), 7.72 (d, J = 8.7 Hz, 1H); LC-MS: m/z 360 $[M+H]^+$; HRMS calcd for $(M+H)^+$ 360.0733, found 360.0733; Anal. ($C_{15}H_{13}ClF_3N_3O_2$) C, H, N.

2-Chloro-4-((1*S*,7*S*,7a*R*)-7-hydroxy-3-oxo-1-(trifluoromethyl)-tetrahydro-1*H*-pyrrolo[1,2-*e*]imidazol-2(3*H*)-yl)-3-methylbenzonitrile (12b). ^{1}H NMR (CD_3OD) δ 1.88−2.01 (m, 1H), 2.25 (ddd, J = 20.3, 7.7, 5.5 Hz, 1H), 2.35 (s, 3H), 3.31−3.35 (m, 1H), 3.63 (ddd, J = 11.1, 7.7, 7.6 Hz, 1H), 4.11 (dd, J = 8.5, 6.9 Hz, 1H), 4.50 (q, J = 6.6 Hz, 1H), 5.17 (br s, 1H), 7.50 (br s, 1H), 7.71 (d, J = 8.2 Hz, 1H); HRMS calcd for $(M+H)^+$ 360.0727, found 360.0726; Anal. ($C_{15}H_{13}ClF_3N_3O_2$) C, H, N.

2-Chloro-4-((1*R*,7*R*,7a*R*)-7-hydroxy-3-oxo-1-(trifluoromethyl)-tetrahydro-1*H*-pyrrolo[1,2-*e*]imidazol-2(3*H*)-yl)-3-methylbenzonitrile (12c). HPLC purity 99%; ^{1}H NMR (CD_3OD) δ 2.03−2.22 (m, 2H), 2.34 and 2.42 (s, total 3H), 3.23 (ddd, J = 10.3, 10.3, 1.9 Hz, 1H), 3.68 (ddd, J = 10.2, 9.3, 9.1 Hz, 1H), 3.94 and 3.99 (t, J = 2.7 Hz, total 1H), 4.31 (t, J = 3.0 Hz, 1H), 5.07 (ddd, J = 13.7, 7.1, 2.2 Hz, 1H), 7.31 and 7.49 (d, J = 8.2 Hz, total 1H), 7.69 (d, J = 8.2 Hz, 1H); HRMS calcd for $(M+H)^+$ 360.0727, found 360.0731; Anal. ($C_{15}H_{13}ClF_3N_3O_2$) Cl.

2-Chloro-4-((1*R*,7*R*,7a*R*)-7-hydroxy-1-isopropyl-3-oxo-tetrahydro-1*H*-pyrrolo[1,2-*e*]imidazol-2(3*H*)-yl)-3-methylbenzonitrile (13). ^{1}H NMR (CD_3OD) δ 0.42 and 0.45 (d, J = 6.6 Hz, total 3H), 1.03 and 1.08 (m, J = 6.6 Hz, total 3H), 1.92−2.07 (m, 2H), 2.32 and 2.41 (s, total 3H), 2.45−2.54 (m, 1H), 2.63 (dddd, J = 9.9, 6.5, 6.5, 3.5 Hz, 1H), 3.13−3.20 (m, 1H), 3.67−3.77 (m, 2H), 4.12 (dd, J = 10.2, 8.0 Hz, 1H), 4.43 and 4.52 (br s, total 1H), 7.38 and 7.42 (dd, J = 8.3, 3.5 Hz, total 1H), 7.65 (dd, J = 8.3, 3.5 Hz, 1H); MS: m/z 665 $[2M-H]^-$; HRMS calcd for $(M+H)^+$ 334.1322, found 334.1333. Anal. ($C_{17}H_{20}ClN_3O_2$) C, H, N.

2-Chloro-4-((7*S*,7a*R*)-7-hydroxy-1-methyl-3-oxo-5,6,7,7a-tetrahydro-3*H*-pyrrolizin-2-yl)-3-methylbenzonitrile (14). Step 1. Amide **26**. To compound **19** (480 mg, 1.4 mmol) was added 10% TFA/CH_2Cl_2 solution (7 mL) at room temperature, and the mixture was stirred for 4 h. Toluene (7 mL) was added, and the reaction was concentrated to give a pale brown residue which was then dissolved in CH_2Cl_2 (5 mL). A solution of PyBrop (1.2 g, 2.5 mmol) and acid **25** (210 mg, 1 mmol) in THF (3 mL) was added followed by *i*-Pr_2NEt (0.52 mL, 3 mmol), and stirring was continued for 3 h at room temperature. The reaction was concentrated and then diluted with EtOAc. The organic layer was washed with water, dried (Na_2SO_4), and concentrated. Purification by silica gel chromatography, eluting with 30% EtOAc in hexanes, provided **26** (220 mg, 36%). ^{1}H NMR ($CDCl_3$) δ 0.08 and 0.10 (s, total 3H), 0.09 and 0.11 (s, total 3H), 0.86 (s, 9 H), 1.91 (dddd, J = 12.8, 6.2, 3.3, 3.0 Hz, 1H), 2.07 (dddd, J = 13.0, 8.8, 8.8, 4.1 Hz, 1H), 2.24 and 2.26 (s, total 3H), 2.27 and 2.31 (s, total 3H), 3.68 (dd, J = 8.8, 3.3 Hz, 2H), 3.66−3.78 (m, 2H), 4.27 and 4.33 (ddd, J = 4.0, 2.1, 2.1 Hz, 1H), 4.48 (s, 1H), 7.08 and 7.17 (d, J = 7.7 Hz, total 1H), 7.41 and 7.44 (d, J = 7.7 Hz, total 1H); LC/MS (ES) m/z 435 $[M+H]^+$.

Step 2. Cyclization and Dehydration. To a 15 mL pressure reaction vessel containing **26** (210 mg, 0.48 mmol) in anhydrous THF (8 mL) was added piperidine (0.24 mL, 2.4 mmol). The vessel was sealed, heated at 100 °C for 15 h, and cooled to room temperature. Purification by silica gel chromatography, eluting with 10−30% EtOAc in hexanes, provided TBS-protected **14** (15 mg, 7%). ^{1}H NMR ($CDCl_3$) δ 0.06 (s, 3H), 0.08 (s, 3H), 0.87 (s, 9 H), 1.98 (s, 3H), 1.99−2.06 (m, 1H), 2.15 (dt, J = 20.3, 6.5 Hz, 1H), 2.48 (s, 3H), 3.80 (ddd, J = 11.6, 7.3, 6.2 Hz, 1H), 3.91 (d, J = 4.4 Hz, 1H), 4.42 (q, J = 5.3 Hz, 1H), 4.45 (br s, 1H), 7.06 and 7.13 (d, J = 7.9 Hz, total 1H), 7.46 and 7.51 (d, J = 7.9 Hz, total 1H); LC-MS m/z 417 $[M+H]^+$.

Step 3. Compound **14**. To TBS-protected **14** (14 mg, 0.036 mmol) in anhydrous THF (0.3 mL) in a plastic vial was added HF pyridine (0.05 mL), and the reaction was stirred at room temperature overnight. The reaction was concentrated and purified by reverse phase preparative HPLC to provide **14** (8 mg, 73%) as a white solid. HPLC purity 95%.; ^{1}H NMR ($CDCl_3$) δ 1.98 and 2.03 (s, total 3H), 2.16−2.34 (m, 1H), 2.22 and 2.29 (s, total 3H), 2.50−2.60 (m, 1H), 3.40−3.50 (m, 1H), 3.63 (ddd, J = 16.8, 11.8, 8.3 Hz, 1H), 3.85−3.97 (m, 1H), 4.06 (d, J = 7.5 Hz, 1H), 4.09 (d, J = 7.5 Hz, 1H), 7.05 and 7.13 (d, J = 8.3 Hz, total 1H), 7.52 (t, J = 7.7 Hz, 1H); LC-MS m/z 303 $[M+H]^+$; HRMS calcd for $[M+H]^+$ 303.0900, found 303.0898.

Androgen receptor binding, functional assays, and an in vivo pharmacological rat model have been reported previously.[28]

Molecular Modeling and Docking. Molecular modeling and docking were performed using ICM software.[48,49] The docking of ligands into AR LBD was performed in a two-step process. Initial docking was carried out using multiple grid representation of the receptor and flexible ligand. Five grid potentials were used to describe the shape, hydrophobicity, electrostatics, and hydrogen-bonding potential of AR LDB. The ligand conformations from the grid-based docking were then optimized with a full atom representation of the receptor and flexible ligand, using ICM stochastic global optimization algorithm.

Acknowledgment. The authors would like to thank Gerry Everlof for performing aqueous solubility and log *P* determination, and James Johnson for conducting exploratory Ames assay.

Supporting Information Available: Preparation of intermediate compounds **16**, **17a**, **17b**, **23**, and **25**. This material is available free of charge via the Internet at http://pubs.acs.org.

References

(1) Feldman, H. A.; Longcope, C.; Derby, C. A.; Johannes, C. B.; Araujo, A. B.; Coviello, A. D.; Bremner, W. J.; McKinlay, J. B. Age Trends in the Level of Serum Testosterone and Other Hormones in Middle-aged Men: Longitudinal Results From the Massachusetts Male Aging Study. *J. Clin. Endocrinol. Metab.* **2002**, *87*, 589−598.

(2) Matsumoto, A. M. Andropause: Clinical Implications of the Decline in Serum Testosterone Levels with Aging in Men. *J. Gerontol.* **2002**, *57A*, M76−M99.

(3) Kaufman, J. M.; Vermeulen, A. The Decline of Androgen Levels in Elderly Men and its Clinical and Therapeutic Implications. *Endocrine Rev.* **2005**, *26*, 833−876.

(4) Gillet, M. J.; Martins, R. N.; Clarnette, R. M.; Chubb, S. A.; Bruce, D. G.; Yeap, B. B. Relationship Between Testosterone, Sex Hormone Binding Globulin and Plasma Amyloid beta Peptide 40 in Older Men with Subjective Memory Loss or Dementia. *J. Alzheimers Dis.* **2003**, *5*, 267−269.

(5) Snyder, P. J.; Peachey, H.; Hannoush, P.; Berlin, J. A.; Loh, L.; Lenrow, D. A.; Holmes, J. H.; Dlewati, A.; Santanna, J.; Rosen, C. J.; Strom, B. L. Effect of Testosterone Treatment on Body Composition and Muscle Strength in Men Over 65 Years of Age. *J. Clin. Endocrinol. Metab.* **1999**, *84*, 2647−2653.

(6) Ferrando, A. A.; Sheffield-Moore, M.; Yeckel, C. W.; Gilkison, C.; Jiang, J.; Achacosa, A.; Lieberman, S. A.; Tipton, K.; Wolfe, R. R.; Urban, R. J. Testosterone Administration to Older Men Improves Muscle Function: Molecular and Physiological Mechanisms. *Am. J. Physiol. Endocrinol. Metab.* **2002**, *282*, E601−E607.

(7) Schroeder, E. T.; Singh, A.; Bhasin, S.; Storer, T. W.; Azen, C.; Davidson, T.; Martinez, C.; Sinha-Hikim, I.; Jaque, S. V.; Terk, M.; Sattler, F. R. Effects of an Oral Androgen on Muscle and Metabolism in Older, Community-dwelling Men. *Am. J. Physiol. Endocrinol. Metab.* **2003**, *284*, E120−E128.

(8) Bhasin, S.; Woodhouse, L.; Casaburi, R.; Singh, A. B.; Mac, R. P.; Lee, M.; Yarasheski, K. E.; Sinha-Hikim, I.; Dzekov, C.; Dzekov, J.; Magliano, L.; Storer, T. W. Older Men are as Responsive as Young Men to the Anabolic Effects of Graded Doses of Testosterone on Skeletal Muscle. *J. Clin. Endocrinol. Metab.* **2005**, *90*, 678−688.

(9) Page, S.; Amory, J. K.; Bowman, F. D.; Anawalt, B. D.; Matsumoto, A. M.; Bremner, W. J.; Tenover, J. L. Exogenous Testosterone (T) Alone or in Combination with Finasteride Increases Physical Performance, Grip Strength, and Lean Body Mass in Older Men with Low Serum T. *J. Clin. Endocrinol. Metab.* **2005**, *90*, 1502−1510.

(10) Gruenwald, D. A.; Matsumoto, A. M. Testosterone Supplementation Therapy for Older Men: Potential Benefits and Risks. *J. Am. Geriat. Soc.* **2003**, *51*, 101−115.

(11) Rhoden, E. L.; Morgentaler, A. Risks of Testosterone-replacement Therapy and Recommendations for Monitoring. *N. Engl. J. Med.* **2004**, *350*, 482−492.

(12) Zhi, L.; Martinborough, E. Selective Androgen Receptor Modulators (SARMs). *Annu. Rep. Med. Chem.* **2001**, *36*, 169−180.

(13) Chengalvla, M.; Oh, T.; Roy, A. K. Selective Androgen Receptor Modulators. *Expert Opin. Ther. Pat.* **2003**, *13*, 59−66.

(14) Gao, W.; Bohl, C. E.; Dalton, J. T. Chemistry and Structural Biology of Androgen Receptor. *Chem. Rev.* **2005**, *105*, 3352−3370.

(15) Omwancha, J.; Brown, T. R. Selective androgen receptor modulators: in pursuit of tissue-selective androgens. *Curr. Opin. Invest. Drugs* **2006**, *7*, 873−881.

(16) Cadilla, R.; Turnbull, P. Selective Androgen Receptor Modulators in Drug Discovery: Medicinal Chemistry and Therapeutic Potential. *Curr. Top. Med. Chem.* **2006**, *6*, 245−270.

(17) Wilson, E. M. Muscle-Bound? A Tissue-Selective Nonsteroidal Androgen Receptor Modulator. *Endocrinology* **2007**, *148*, 1−3.

(18) Gao, W.; Dalton, J. T. Expanding the therapeutic use of androgens via selective androgen receptor modulators (SARMs). *Drug Discovery Today* **2007**, *12*, 241−248.

(19) Hamann, L. G.; Mani, N. S.; Davis, R. L.; Wang, X. N.; Marschke, K. B; Jones, T. K. Discovery of a Potent, Orally Active, Nonsteroidal Androgen Receptor Agonist: 4-Ethyl-1,2,3,4-tetrahydro-6-(trifluoromethyl)-8-pyridono[5,6-*g*]quinoline (LG121071). *J. Med. Chem.* **1999**, *42*, 210−212.

(20) Oeveren, A. V.; Motamedi, M.; Mani, N. S.; Marschke, K. B.; López, F. J.; Schrader, W. T.; Negro-Vilar, A.; Zhi, L. Discovery of 6-*N*,*N*-Bis(2,2,2-trifluoroethyl)amino-4-trifluoromethylquinolin-2(1*H*)-one as a Novel Selective Androgen Receptor Modulator *J. Med. Chem*. **2006**, *49*, 6143−6146.

(21) Marhefka, C. A.; Gao, W.; Chung, K.; Kim, J.; He, Y.; Yin, D.; Bohl, C.; Dalton, J. T.; Miller, D. D. Design, Synthesis and Biological Characterization of Metabolically Stable Selective Androgen Receptor Modulators. *J. Med. Chem.* **2004**, *47*, 993−998.

(22) Van Dort, M. E.; Robins, D. M.; Wayburn, B. Design, Synthesis, and Pharmacological Characterization of 4-[4,4-Dimethyl-3-(4-hydroxybutyl)-5-oxo-2-thioxo-1-imidazolidinyl]-2-iodobenzonitrile as a High-Affinity Nonsteroidal Androgen Receptor Ligand. *J. Med. Chem*. **2000**, *43*, 3344−3347.

(23) Chen, J.; Hwang, J. D.; Bohl, C. E.; Miller, D. D.; Dalton, J. T. A Selective Androgen Receptor Modulator for Hormonal Male Contraception. *J. Pharmacol. Exp. Ther.* **2005**, *312*, 546−553.

(24) Kim, J.; Wu, D.; Hwang, D. J.; Miller, D. D.; Dalton, T. T. The Para Substituent of *S*-3-(Phenoxy)-2-hydroxy-2-methyl-*N*-(4-nitro-3-trifluoromethyl-phenyl)-propionamides Is a Major Structural Determinant of in Vivo Disposition and Activity of Selective Androgen Receptor Modulators. *J. Pharmacol. Exp. Ther.* **2005**, *315*, 230−239.

(25) Gao, W.; Reiser, P. J.; Coss, C. C.; Phelps, M. A.; Kearbey, J. D.; Miller, D. D.; Dalton, J. T. Selective Androgen Receptor Modulator Treatment Improves Muscle Strength and Body Composition and Prevents Bone Loss in Orchidectomized Rats. *Endocrinology* **2005**, *146*, 4887−4897.

(26) Chen, J.; Hwang, D. J.; Chung, K.; Bohl, C. E.; Fisher, S. J.; Miller, D. D.; Dalton, J. T. In Vitro and in Vivo Structure-Activity Relationships of Novel Androgen Receptor Ligands with Multiple Substituents in the B-Ring. *Endocrinology* **2005**, *146*, 5444−5454.

(27) Hanada, K.; Furuya, K.; Yamamoto, N.; Nejishima, H.; Ichikawa, K.; Nakamura, T.; Miyakawa, M.; Amano, S.; Sumita, Y.; Oguro, N. Bone anabolic effects of S-40503, a novel nonsteroidal selective androgen receptor modulator (SARM), in rat models of osteoporosis. *Biol. Pharm. Bull.* **2006**, *26*, 1563−1569.

(28) Ostrowski, J.; Driscoll, J. E.; Lupisella, J. A.; Manfredi, M. C.; Beehler, B. C.; Bi, Y.; Sun, C.; Seethala, R.; Golla, R.; Sleph, P. G.; Fura, A.; Narasimhan, N.; Krystek, S. R., Jr.; An, Y.; Kish, K. F.; Sack, J. S.; Bonacorsi, S. J.; Cao, K.; Mookhtiar, K. A.; Grover, G. J.; Hamann, L. G. Pharmacological and X-ray Structural Characterization of a Novel Selective Androgen Receptor Modulator: Potent Hyperanabolic Stimulation of Skeletal Muscle with Hypostimulation of Prostate in Rats. *Endocrinology* **2007**, *148*, 4−12.

(29) Sun, C.; Robl, A. J.; Wang, C. T.; Huang, Y.; Driscoll, J. E.; Lupisella, J. A.; Beehler, B. C.; Golla, R.; Sleph, P. G.; Seethala, R.; Fura, A.; Krystek, S. R., Jr.; An, Y.; Malley, M.; Sack, J. S.; Salvati, M. E.; Grover, G. J.; Ostrowski, J.; Hamann, L. G. Discovry of Potent, Orally-Active and Muscle-Selective Androgen Receptor Modulators (SARMs) Based on an *N*-Aryl-hydroxybicyclohydantoin Scaffold. *J. Med. Chem*. **2006**, *49*, 7596−7599.

(30) Hamann, L. G.; Manfredi, M. C.; Sun, C.; Krystek, S. R., Jr.; Huang, Y.; Bi, Y. Augeri, D. J.; Wang, T.; Zou, Y.; Betebenner, D. A.; Fura, A.; Seethala, R.; Golla, R.; Kuhns, J. E.; Lupisella, J. A.; Darienzo, C. J.; Custer, L. L.; Price, J. L.; Johnson, J. M.; Biller, S. A.; Zahler, R.; Ostrowski, J. Tandem optimization of target activity and elimination of mutagenic potential in a potent series of *N*-aryl bicyclic hydantoin-based selective androgen receptor modulators. *Bioorg. Med. Chem. Lett*. **2007**, *17*, 1860−1864.

(31) Synthesis and SAR of novel hydantoin derivatives as selective androgen receptor modulators. Zhang, X.; Allan, G. F.; Sbriscia, T.; Linton, O.; Lundeen, S. G.; Sui, Z. *Bioorg. Med. Chem. Lett*. **2006**, *16*, 5763−5766.

(32) Zhang, X.; Li, X.; Allan, G. F.; Sbriscia, T.; Linton, O.; Lundeen, S. G.; Sui, Z. Serendipitous Discovery of Novel Imidazolopyrazole Scaffold as Selective Androgen Receptor Modulators. *Bioorg. Med. Chem. Lett*. **2007**, *17*, 439−443.

(33) Synthesis of potent and tissue-selective androgen receptor modulators (SARMs): 2-(2,2,2)-trifluoroethyl-benzimidazole scaffold. Ng, R. A.; Lanter, J. C.; Alford, V. C.; Allan, G. F.; Sbriscia, T.; Lundeen, S. G.; Sui, Z. *Bioorg. Med. Chem. Lett*. **2007**, *17*, 1784−1787.

(34) van Oeveren, A.; Pio, B.; Tegley, C. M.; Higuchi, R. I.; Wu, M.; Jones, T. K.; Marschke, K. B.; Negro-Vilar, A.; Zhi, L. Discovery of an androgen receptor modulator pharmacophore based on 2-quinolinones. *Bioorg. Med. Chem. Lett*. **2007**, *17*, 1523−1526.

(35) Miner, J. N.; Chang, W.; Chapman, M. S.; Finn, P. D.; Hong, M. H.; López, F. J.; Viveros, K. H.; Zhi, L.; Negro-Vilar, A. An Orally Active Selective Androgen Receptor Modulator Is Efficacious on Bone, Muscle, and Sex Function with Reduced Impact on Prostate. *Endocrinology* **2007**, *148*, 363−373.

(36) van Oeveren, A.; Motamedi, M.; Martinborough, E.; Zhao, S.; Shen, Y.; West, S.; Chang, W.; Kallel, A.; Marschke, K. B.; Lopez, F. J.; Negro-Vilar, A.; Zhi, L. Novel selective androgen receptor modulators: SAR studies on 6-bisalkylamino-2-quinolinones. *Bioorg. Med. Chem. Lett*. **2007**, *17*, 1527−1531.

(37) Luh, T-Y.; Chow, H-F.; Leung, W. Y.; Tam, S. W. On the Regioselectivity of the Beckmann Rearrangement of Cyclobutanones with *O*-Mesitylene Sulfonylhydroxylamine. A Convenient Synthesis of Substituted Octahydrocyclopenta[*b*]pyrroles. *Tetrahedron Lett*. **1985**, *41*, 519−525.

(38) Marcoux, J-F.; Wagaw, S.; Buchwald, S. L. Palladium-Catalyzed Amination of Aryl Bromides: Use of Phosphinoether Ligands for the Efficient Coupling of Acyclic Secondary Amines. *J. Org. Chem*. **1997**, *62*, 1568−1569.

(39) Pi, Z.; Huang, Y.; Sun, C.; Sutton, J. C.; Hamann, L. G. Unpublished results.

(40) Sack, J. S.; Kish, K. F.; Wang, C; Attar, R. M.; Kiefer, S. E.; An, Y.; Wu, G. Y.; Scheffler, J. E.; Salvati, M. E.; Krystek, S. R., Jr.; Weinmann, R.; Einspahr, H. M. Crystallographic structures of the ligand-binding domains of the androgen receptor and its T877A mutant complexed with the natural agonist dihydrotestosterone *Proc. Natl. Acad. Sci.* **2001**, *98*, 4904−4909.

(41) Solid state form for **3** (crystalline), **8** (crystalline), **10a** (crystalline), **11a** (partial crystalline), and **12d** (amorphous). The HPLC measured log *P*/*D* value for **3** (1.3), **8** (1.3), **10a** (2.2), **11a** (2.7), and **12d** (2.3). The mp for **3** (255−257 °C), **8** (197−198.5 °C), **10a** (175−177 °C), **11a** (125−126.5 °C), and **12d** (99−101 °C).

(42) Beyler, A. L.; Arnold, A.; Potts, G. O. Method for Evaluating Anabolic and Catabolic Agents in Laboratory Animals. *J. Am. Med. Women's Assoc.* **1968**, *23*, 708−712.

(43) Chinoy, N. L.; Sheth, K. M.; Shah, V. C. A Comparative Histophysiological Study on the Normal, Castrated and Testosterone-treated Levator Ani Muscle of Rodents. *Acta Endocrinol.* **1973**, *74*, 389−398.
(44) The ED_{50} is defined as the dose required to produce a 50% recovery of muscle or prostate tissues as compared to intact sham-operated control group.
(45) Pharmacokinetics study of **11a** in rat was dosed at 5 mg/kg (i.v.) and 10 mg/kg (p.o.). $F\% = 65\%$, $T_{1/2} = 5.5$ h, $C_{max} = 2.1$ μM (p.o.) , $T_{max} = 0.8$ h (p.o.), total body clearance 58 mL/min/kg.
(46) PR, ERα, ERβ, GR binding $K_i > 10$ μM; SHBG binding $K_i > 100$ μM; aromatase inhibition $IC_{50} > 100$ μM. Human hepatotoxicity assay $IC_{50} > 200$ μM. CYP450 isozymes 2C19 $IC_{50} = 7.6$ μM; 1A2, 2C9, 2D6, 3A4 $IC_{50} > 40$ μM. Patch clamp hERG = 6% at 30 μM.
(47) Zeiger, E. Carcinogenicity of Mutagens: Predictive Capability of the Salmonella Mutagenesis Assay for Rodent Carcinogenicity. *Cancer Res.* **1987**, *47*, 1287.
(48) ICM Program Manual, version 2.8 (2000), Molsoft, San Diego, CA.
(49) Totrov, M.; Abagyan, R. Flexible Protein-Ligand Docking by Global Energy Optimization in Internal Coordinates. *Proteins Suppl*. **1997**, *1*, 215−220.

JM070312D